

# Comparison of some properties of neodymium-doped silica glasses prepared by sol-gel and melting

M. G. FERREIRA DA SILVA

*Departamento de Engenharia Cerâmica e do Vidro, UIMC, Universidade de Aveiro 3810 Aveiro, Portugal*  
E-mail: *gsilva@cv.ua.pt*

M. A. VALENTE

*Departamento de Física, Universidade de Aveiro, 3810 Aveiro, Portugal*  
E-mail: *mav@fis.ua.pt*

Samples with  $10\text{Nd}_2\text{O}_3 \cdot 5\text{CaO} \cdot 17\text{Al}_2\text{O}_3 \cdot 68\text{SiO}_2$  composition (mol %) were prepared by the sol-gel method and by melting. The structure of the samples was investigated by X-ray diffraction, scanning electron microscopy, infrared spectroscopy, a.c. susceptibility measurements and electron spin resonance. The gel-derived sample heat-treated between 250 and 700°C is amorphous and has a granular microstructure. In the samples heat-treated at 800, 900 and 1000°C we detected by X-ray diffraction  $\text{AlNdO}_3$  crystalline particles. The melted sample was amorphous and the micrograph shows a glass matrix containing particles. The infrared measurements show structural changes produced by the heat-treatment of the gel samples. The magnetic susceptibility data indicates that neodymium oxide is present in these samples as  $\text{Nd}^{3+}\text{-O-Nd}^{3+}$  aggregates with an antiferromagnetic interaction. © 2001 Kluwer Academic Publishers

## 1. Introduction

The optical properties of rare-earth doped glasses are affected by the glass forming anions and glass forming/modifying cations and to a lesser extent by the methods of preparation and heat-treatment [1]. The distribution of  $\text{Nd}^{3+}$  ions in a host glass affects the fluorescent lifetime of  $\text{Nd}^{3+}$ . In Nd-Al co-doped silica glasses the homogeneity of the distribution of  $\text{Nd}^{3+}$  can be increased and the clustering of  $\text{Nd}^{3+}$  controlled [2]. The sol-gel method has been successfully applied to the synthesis of neodymium silica-glasses with  $\text{Nd}^{3+}$  content greater than is attainable by conventional processing technique [3].

In this paper  $10\text{Nd}_2\text{O}_3 \cdot 17\text{Al}_2\text{O}_3 \cdot 5\text{CaO} \cdot 68\text{SiO}_2$  (mol%) glasses were prepared by the sol-gel method and by melting. We chose this composition because the performance of a laser glass is linked to the rare earth doping level and the distribution of  $\text{Nd}^{3+}$  ions, (which is influenced by the presence of aluminium). In this study we compare the structure and magnetic properties of the gel and melted glasses and we prove that by using the sol-gel method the distribution of  $\text{Nd}^{3+}$  is random and the formation of  $\text{Nd}^{3+}$  clusters is reduced.

## 2. Experimental

Samples of  $10\text{Nd}_2\text{O}_3 \cdot 5\text{CaO} \cdot 17\text{Al}_2\text{O}_3 \cdot 68\text{SiO}_2$  (mol %) were prepared by two methods: sol-gel and melting. The samples obtained by the sol-gel route were pre-

pared from tetraethylorthosilicate (TEOS), aluminium (III) nitrate nonahydrate ( $\text{Al}(\text{NO}_3)_3 \cdot 9\text{H}_2\text{O}$ ), neodymium (III) nitrate hexahydrate ( $\text{Nd}(\text{NO}_3)_3 \cdot 6\text{H}_2\text{O}$ ), and calcium nitrate tetrahydrate ( $\text{Ca}(\text{NO}_3)_2 \cdot 4\text{H}_2\text{O}$ ) as sources of silica, neodymium, alumina and calcium oxides. First, a mixture of TEOS, ethanol, water and HCl in a molar ratio 1 : 1 : 1 : 0.0027 was stirred for one hour at room temperature. After this hydrolysis, nitrates which had been dissolved in water (1 ml  $\text{H}_2\text{O}$  for each gram of nitrate) were added. The solution was stirred for one hour, poured into Petri dishes and allowed to gel and dried at 60°C. The gel obtained was then heat-treated at temperatures between 250 and 1000°C in oxidizing conditions (air).

The melted glass was prepared by mixing appropriate amounts of  $\text{SiO}_2$ ,  $\text{CaCO}_3$ ,  $\text{Nd}_2\text{O}_3$  and  $\text{Al}_2\text{O}_3$ . Melting was carried out in a corundum crucible, at about 1700°C, in air. The glass was then quenched in air. For increasing homogeneity melting at higher temperature may be suitable to increase the homogeneity of the final glass [4]. The structure and properties of the samples were examined by X-ray diffraction (XRD), scanning electron microscopy (SEM), infrared spectroscopy (FT-IR), electron paramagnetic resonance (EPR) and ac susceptibility measurements ( $\chi$  a.c.).

XRD analysis was performed at room temperature on a Rigaku XDMAX diffractometer using monochromated (monochromator graphite)  $\text{Cu K}\alpha$  radiation ( $\lambda = 1.5418 \text{ \AA}$ ) at 40 kV and 30 mA, by step scanning

using powdered samples. We used three seconds for each step of counting time and the step width was  $0.05^\circ$ .

The SEM micrographs were obtained using an electron microscope (Hitachi (S4100-1)).

The infrared transmission spectra were recorded from, 400 to  $4000\text{ cm}^{-1}$ , in a spectrometer (Mattson 7000 (FTIR)). The FT-IR samples were prepared using the KBr pellet method.

The alternating current magnetic susceptibility ( $\chi$  a.c.) measurement, between 80 and 320 K, was done at 119.5 Hz in a magnetic field of 10 gauss. The measurements were performed on a home-built mutual inductance differential transformer system. The accuracy of temperature control and measurements was  $<\pm 0.1\text{ K}$  over the whole range and the overall accuracy of measurements of the magnetic moment is better than  $\pm 0.2\%$ .

The EPR measurements were carried out in a spectrometer (Brüker ESP 300E) operating at X band (9.7 GHz). The EPR spectra were acquired at 5, 50 and 300 K on finely powdered samples packed in quartz capillary tubes. The spectrometer parameters were the following: power = 20.1 mW, modulation amplitude =  $10^{-4}$  Tesla, modulation of frequency = 100 kHz, field sweeps of  $5 \times 10^{-2}$  to  $4.5 \times 10^{-1}$  Tesla, receiver gain =  $10^5$ .

$^{27}\text{Al}$  NMR (Nuclear Magnetic Resonance) spectra were not registered because as referred by T. Fujiyama *et al.* [5], when aluminium ions are connected with neodymium through an Al-O-Nd bond the NMR peaks disappear.

### 3. Results

#### 3.1. X-ray diffraction (XRD)

The gel-derived sample heat-treated between 250 and  $700^\circ\text{C}$  and the melted glass are amorphous (Fig. 1A).

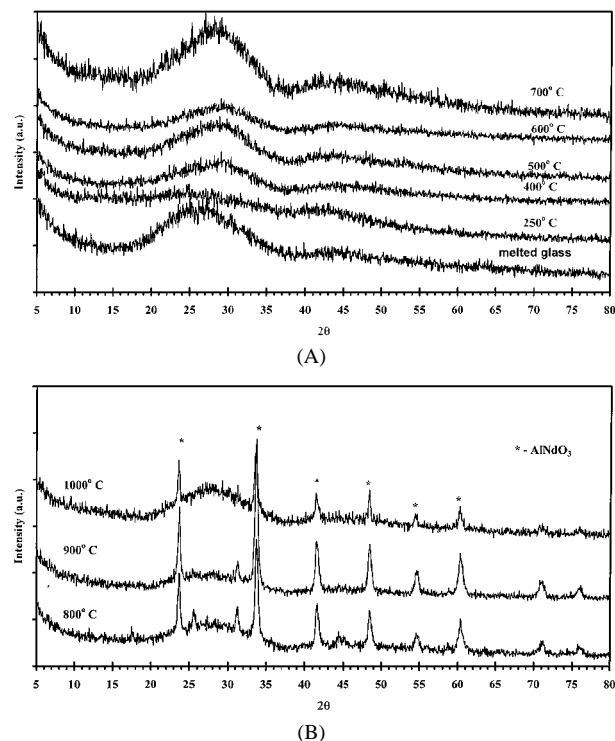


Figure 1 (A) X-ray diffraction patterns of the sol-gel samples heat-treated at 250, 400, 500, 600,  $700^\circ\text{C}$  and the melted sample. (B) X-ray diffraction patterns of the sol-gel samples heat-treated at 800, 900 and  $1000^\circ\text{C}$ .

In the samples heat-treated at 400, 500, 600 and  $700^\circ\text{C}$  we observed a band that shifts to smaller  $2\theta$  when the temperature increases (Fig. 1A). The X-ray diffraction of a melted sample was similar to that obtained for the  $700^\circ\text{C}$  sol-gel sample (Fig. 1A).

However, in the sample treated at 800, 900 and  $1000^\circ\text{C}$  we detected the presence of  $\text{AlNdO}_3$  (aluminium neodymium oxide) (Fig. 1B).

#### 3.2. Scanning electron microscopy

The SEM micrographs of the gel-derived samples are shown in Figs 2 and 3. The fractured surfaces of 250, 500 and  $700^\circ\text{C}$  samples present a granular microstructure (Fig. 2A). However, in the as prepared surface of the 500 and  $700^\circ\text{C}$  samples the coalescence of the particles is observed (Fig. 2B). At  $1000^\circ\text{C}$  the granular structure disappears and we can see a densified material (Fig. 3A) and in some regions crystalline particles are observed (Fig. 3B). In the fractured surface of a melted sample we detected the presence of particles in a glass matrix (Fig. 4).

#### 3.3. FT-IR spectra

The FT-IR spectra of gel-derived samples and glasses prepared by melting are shown in Fig. 5.

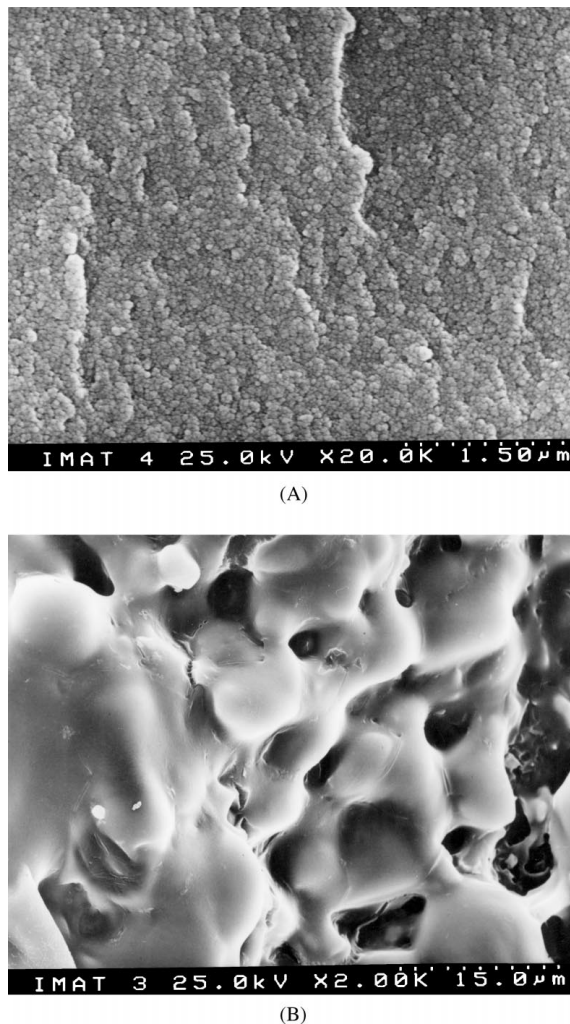
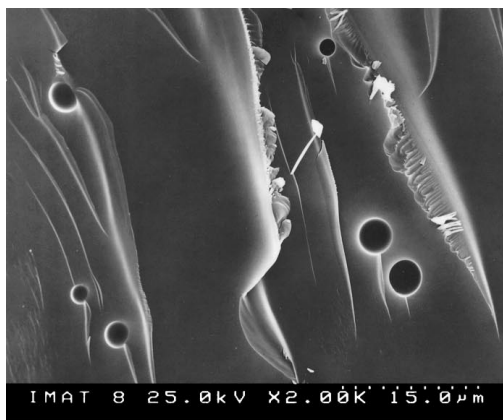


Figure 2 Scanning electron micrograph of the samples: (A) fractured surface of the  $500^\circ\text{C}$  sample; (B) free surface of the  $500^\circ\text{C}$ -sample.



(A)



(B)

Figure 3 Scanning electron micrograph of the 1000°C sample; (A) fractured surface (B) crystalline particles in the fractured surface.

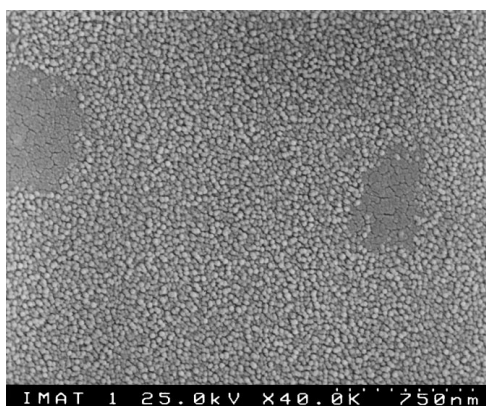


Figure 4 SEM of the melted sample (fractured surface).

The gel-derived sample spectra have a band at  $3440\text{ cm}^{-1}$ , that is due to Si-OH stretching vibrations [6, 7] and a band near  $1640\text{ cm}^{-1}$  that is attributed to the deformation vibration of free water [8, 9]. The intensity of these bands decreases when the heat treatment temperature increases. The band around  $1480\text{ cm}^{-1}$  is due to C-H bending vibrations [9, 10] and is not present in the samples heat-treated at temperature greater than  $250^\circ\text{C}$ . The band near  $1060\text{ cm}^{-1}$  can be assigned to the stretching vibration of Si-O bonds [11, 12] and shifts to smaller wavenumbers when the heat-treatment temperature increases (between  $250$  and  $700^\circ\text{C}$ ). However, this band in the spectra samples at  $1000^\circ\text{C}$ , shifts to

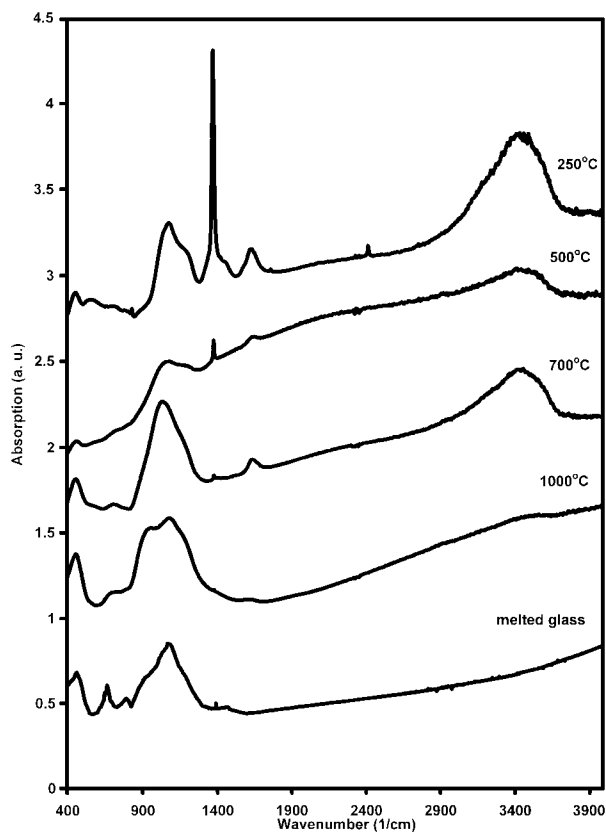


Figure 5 Infrared absorption spectra of the sol-gel derived samples ( $250$ ,  $500$ ,  $700$ ,  $1000^\circ\text{C}$ ) and of the melted glass.

higher wavenumber. The band around  $920\text{ cm}^{-1}$ , that appears in the spectrum of the  $1000^\circ\text{C}$ -sample (Fig. 5), may be due to the formation of  $\text{AlNdO}_3$  and the band at  $\sim 680\text{ cm}^{-1}$  to the presence of  $\text{AlO}_4$  groups [13]. The vibrational mode of deformation of the Si-O-Si bonds is represented by the band at  $\sim 450\text{ cm}^{-1}$  [6–10]. The amplitude of this band increased with the increase of the temperature of the thermal treatment.

The FT-IR spectrum of the sample prepared by melting (Fig. 5) has absorption bands at  $\sim 1060$ ,  $\sim 680$  and  $\sim 460\text{ cm}^{-1}$ . This spectrum is similar to those obtained for other silicate glasses [13–15]. The first band is assigned to the antisymmetric stretching mode involving bridged oxygen (Si-O-Si bonds) and the other two bands are related to the bonding modes involving bridges oxygens [13–15].

### 3.4. Magnetic susceptibility

The temperature dependence of reciprocal susceptibility ( $\chi^{-1}$ ) is plotted in Fig. 6 for the gel and melted samples from  $80$  to  $300\text{ K}$ . The data are approximately a linear functions of the inverse of temperature indicating that the magnetic susceptibility obeys the Curie-Weiss law

$$\chi = C/(T - \theta_p) \quad (1)$$

Where  $\theta_p$  is the paramagnetic Curie temperature,  $C$  the Curie constant and  $T$  the temperature.  $\theta_p$  is indicative of the strength of the average interaction between the Nd ions and is negative for all the samples which is due antiferromagnetically coupled Nd ions [16]. The other magnetic property calculated from the susceptibility

TABLE I Effective magnetic moment  $\mu_{\text{eff}}$  and paramagnetic Curie-Weiss temperature  $\theta_p$  derived from the data for  $\chi^{-1}$  as a function of temperature for the glasses measured

Heat-treatment Temperature ( $^{\circ}\text{C}$ )	$-\theta_p$ (K) $\pm 2$	$\mu_{\text{eff}}$ ( $\mu\text{B}$ ) $\pm 0.02$
250	56	2.64
500	30	3.19
700	27	3.23
1000	44	3.58
Melting glass	70	3.05

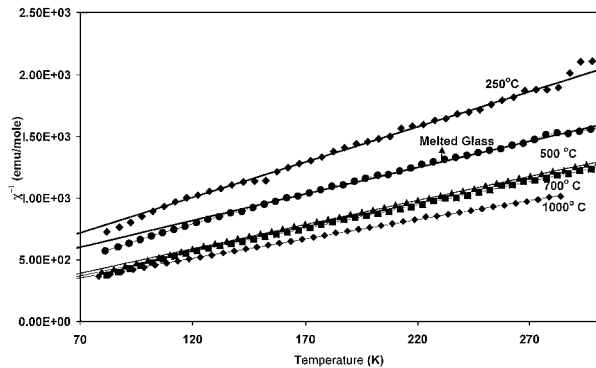


Figure 6 The temperature dependence of the inverse magnetic susceptibility of the sol-gel samples and melted glass.

data is expressed as an effective localised moment  $\mu_{\text{eff}}$  (Table I).

$$\mu_{\text{eff}} = \sqrt{\frac{3\kappa_B C}{N}} \quad (2)$$

Where  $\kappa_B$  is the Boltzmann constant and  $N$  the number of magnetic particles. The  $\mu_{\text{eff}}$ 's for the sol-gel samples increase with increase of the heat-treatment temperature (Table I). The  $\mu_{\text{eff}}$  for all samples, except 1000 $^{\circ}\text{C}$ , is smaller than that for the neodymium free ion ( $3.6 \mu_B$ ) [17].

### 3.5. EPR

For all samples and for all temperatures (5, 50 and 300 K) of measurements EPR absorption was not detected. The electronic spin-lattice relaxation times of non-s-state 4f rare earth ions such as Nd usually preclude the possibility of observing any EPR signal at 77 K [4].

## 4. Discussion

In the XRD patterns (Fig. 1), of the gel sample, the shift of the broad band (to lower  $2\Theta$ ), when the temperature of heat-treatment increases, means that the long-range periodic structure was in formation [11]. The results of FT-IR measurements show some structural changes during the heat-treatment process. The progressive polycondensation of the gel-sample, with the increase of heat-treatment temperature, is indicated by an increase of the amplitudes of the 1040 and 450  $\text{cm}^{-1}$  bands (Fig. 5). The 1480  $\text{cm}^{-1}$  band is only present in the sample heat-treated at 250 $^{\circ}\text{C}$  because, at a temperature between 250 $^{\circ}\text{C}$  and 500 $^{\circ}\text{C}$ , the alkoxy groups are removed by oxidation [9, 10]. The band at  $\sim 1060 \text{ cm}^{-1}$

shifts to smaller wave numbers with increasing temperature due to a softening of the Si-O bonds (between 250 and 700 $^{\circ}\text{C}$ ) [11]. At 1000 $^{\circ}\text{C}$  the band shifts to larger wave numbers due to an increase in the strength of Si-O bonds [11].

From the magnetic susceptibility data (Fig. 6) we conclude that some of the neodymium is present, in these samples, as  $\text{Nd}^{3+}$ -O- $\text{Nd}^{3+}$  aggregates with an antiferromagnetic interaction [18]. We assume that the maximum interaction,  $J$ , between two ions is obtained when two ions share an oxygen at a minimum bond angle. Though this interaction can fluctuate according to the bond angle, in agreement with a qualitative argument that we are following, we can assume an average for  $J$ . Joining  $\text{Nd}^{3+}$ -O- $\text{Nd}^{3+}$  to form an aggregate does not affect the interactions but only the average number,  $N$ , of nearest neighbours. In the mean field theory of magnetic properties, the Curie temperature,  $\theta_p$ , is given by  $\theta_p \approx NJ$  and thus we see that in our case  $\theta_p$  should increase linearly with increases of  $N$  [19]. The  $\theta_p$  (Table I) obtained for the 250 $^{\circ}\text{C}$  - sample can be explained by the existence of aggregates of neodymium oxide particles. The number of neighbours of the neodymium oxide particles seems to be smaller in the case of the 700 $^{\circ}\text{C}$  sample because it has a smaller  $\theta_p$  (Table I). At 1000 $^{\circ}\text{C}$  there is an increase in  $\theta_p$  that we ascribe to the formation of the  $\text{AlNdO}_3$  crystalline particles also detected by XRD, SEM and FT-IR (Figs 1–5). However, the melted sample has a  $\theta_p$  larger than the gel-samples. This larger  $\theta_p$  is attributed to a larger number of Nd oxide particles in the melted samples.

We explain the increase with the heat-treatment temperature of  $\mu_{\text{eff}}$ , for sol-gel samples by the molar mass difference between the 250 and 1000 $^{\circ}\text{C}$  samples. That difference may be due to the fact that we assume the same molar formula,  $10\text{Nd}_2\text{O}_3 \cdot 5\text{CaO} \cdot 17\text{Al}_2\text{O}_3 \cdot 68\text{SiO}_2$ , for all gel-samples and this assumption may be incorrect because the gel-samples have a progressive deshydration, polycondensation and the removal of alkoxy groups. So the actual molar weight is greater for the sample heat-treated at 250 $^{\circ}\text{C}$  and has the lower  $\theta_p$  compared to the  $\theta_p$  of the sample heat-treated at 1000 $^{\circ}\text{C}$ .

The  $\mu_{\text{eff}}$ , of the melted sample, is attributed to a smaller  $C$  (Curie constant). The presence of exchange interactions between magnetic ions, respectively the process of exchange pair formation, affects  $C$ . In view of this process, an increase of the number of antiferromagnetically coupled ion pairs leads to a variation of  $C$  similar to that given by a decrease of the number of magnetic ions.

## 5. Conclusions

From the results it is evident that the distribution of  $\text{Nd}^{3+}$  ions is more uniform in the samples prepared by the sol-gel method.

The magnetic aggregates in the samples have an antiferromagnetic interaction, that is function of the heat-treatment temperature for the sol-gel samples.

## Acknowledgements

Aknowledgment is made to the FCT (Portuguese Foundation for Science and Technology) and the Research

Institut of Aveiro University (Proj.3401) for financial support. The authors also wish thank to Nuno Ferreira and Vera Batel, Conceição Lopes for the preparation of the samples and some technical help.

## References

1. P. NACHIMUTHU, P. HARIKISHAN and R. JAGANNATHAN, *Phys. Chem. Glasses* **38** (1997) 59.
2. T. FUJIYAMA, M. HORI and M. SASAKI, *J. Non-Cryst. Solids* **121** (1990) 273.
3. E. J. A. POPE and J. D. MACKENZIE, *ibid.* **106** (1988) 236.
4. S. SEN and J. F. STEBBINS, *ibid.* **188** (1995) 54.
5. T. FUJIYAMA, T. YOKOYAMA, M. HORI and M. SASAKI, *ibid.* **135** (1991) 198.
6. A. BERTOLUZZA, C. FAGNANO, M. A. MORELLI, V. GOTTARDI and M. GUGLIELMI, *ibid.* **48** (1982) 117.
7. M. NOGAMI and Y. MORYA, *ibid.* **37** (1980) 191.
8. F. PANCAZI, J. PHALIPPOU, F. SORRENTINO and J. ZARZYCKI, *ibid.* **63** (1984) 81.
9. P. MANIER, A. NAROTSKY, A. M. RABINOVICH, D. L. WOOD and N. A. KOPYLOV, *Mat. Res. Soc. Symp. Proc.* **121** (1988) 323.
10. G. ZHAO and N. TOHGE, *Mat. Res. Bulletin* **33**(1) (1998) 21.
11. K. KATO, *J. Mater. Sci.* **26** (1991) 6777.
12. N. P. BANSAL, *J. Am. Ceram. Soc.* **71** (1988) 666.
13. J. ZARZYCKI, "Glasses and the Vitreous State" (Cambridge University, Cambridge, 1991).
14. J. W. PARK and H. CHEN, *J. Non-Cryst. Solids* **40** (1980) 515.
15. J. WONG and C. A. ANGELL, "Glass Structure by Spectroscopy" (Marcel Dekker, New York, 1976).
16. I. ARDELEAN, CH. IONCA and V. SEVIANU, *J. Less. Common Met.* **111** (1985) 113.
17. D. CRAIK, "Magnetism Principles and Applications" (John Wiley & Sons, New York, 1995).
18. D. W. MOON, J. M. AITKEN and R. K. MACCRONE, *Physics and Chemistry of Glasses* **16**(5) (1975) 91.
19. M. A. VALENTE and S. K. MENDIRATTA, *ibid.* **33**(4) (1992) 149.

Received 7 June 1999  
and accepted 22 May 2000